Structural Properties of Four Isomeric C2'/C3' Modified Uridines

Leo H. Koole,[†] Jin-Chang Wu,[†] Stephen Neidle,[‡] and Jyoti Chattopadhyaya*,[†]

Contribution from the Department of Bioorganic Chemistry, Box 581, Biomedical Centre, Uppsala University, S-751 23 Uppsala, Sweden, and the Cancer Research Campaign Biomolecular Structure Unit, The Institute of Cancer Research, Sutton, Surrey SM2 5NG, United Kingdom. Received April 1, 1991

Abstract: Detailed structural analyses on the C2'/C3' modified β-D-uridines **1** [1-(2'-deoxy-2'-C,3'-O-(1-methylethylene)-β-D-*ribo*-furanosyl)uracil], **2** [1-(3'-deoxy-3'-C,2'-O-(1-methylethylene)-β-D-*ribo*-furanosyl)uracil], **3** [1-(2'-deoxy-2'-C,3'-O-(1-methylethylene)-β-D-*lyxo*-furanosyl)uracil], and **4** [1-(3'-deoxy-3'-C,2'-O-(1-methylethylene)-β-D-*lyxo*-furanosyl)uracil] are reported. These compounds feature an additional furanoid ring (B-ring) which bridges C2' and C3', either via the α-face (structures **1** and **2**) or via the β-face of the molecule (structures **3** and **4**). The two furanoid rings in each of the structures **1**–**4** share the C2'–C3' bond and therefore have correlated conformations. Structures **1**–**4** were studied in CDCl₃–CD₃OD (9:1) solution with 500 MHz ¹H NMR. One-dimensional NOE difference spectroscopy was used to assess the stereochemical identity of each of the structures **1**–**4**. The conformational properties of the furanoid rings in **1**–**4** were studied on the basis of the vicinal ¹H–¹H *J* coupling constants. It was found that compound **1** features a South-type puckered ribose ring, while the attached B-ring is in a North-type conformation. The preferred conformation of **2** appears to be opposite: North- and South-type conformations are found for the ribose and B-rings, respectively. The conformational characteristics of the furanose rings in **1** and **2** could not be exactly defined. Rather, we have defined the conformational spaces which are compatible with the experimental data. The NMR derived conformation of structure **2** is found to be in good agreement with the X-ray crystal structure. The NMR data on compounds **3** and **4** merely allowed us to conclude that these systems are engaged in a possibly conformational equilibrium. It is briefly mentioned that the conformational results on **1**–**4** are in perfect agreement with our previous conformational studies on other C2' or C3' modified nucleosides, from which two principles emerged: (i) a nonelectron-withdrawing substituent on C2' or C3' tends to attain a pseudoequatorial location for steric reasons and (ii) an electronegative substituent on C2' or C3' tends to occupy a pseudoaxial site because of the stabilizing gauche effect. It appears that the conformational properties of **1**–**4** are also governed by these simple principles, which now apply to both furanose rings simultaneously.

Introduction

Structurally modified nucleosides have been intensively investigated for more than three decades.[1] The interest in this class of compounds is readily understood if one considers that (i) a variety of modified nucleosides and nucleotides play a vital role in biochemical regulation (e.g., signal function of 3',5'-cyclic nucleotides[1e] and the function of modified aglycons in transfer RNAs),[1f] (ii) some modified nucleosides are active anticancer or antiviral drugs, (iii) new modified nucleosides are continuously identified after isolation from different biological sources, and (iv) preparation of modified nucleosides frequently poses a synthetic challenge since regio- and stereoselective transformations and tedious choice of protective groups are required. Moreover, the interest in the field has substantially increased since the discovery that several modified nucleosides are active against various types of the human immunodeficiency virus.[2]

Our group has a longstanding interest in the synthesis of *furanose-modified* nucleosides.[3] More specifically, we have explored several novel preparative approaches for regio- and stereoselective introduction of substituents on C2' or C3' of the furanose ring. Subsequent conformational studies utilizing ¹H NMR spectroscopy and analysis of *J* coupling constants indicated that both the nature and the exact location of the substituent have a major impact on the conformational properties of the furanose ring.[3c–e,4] Two general principles were recognized: (i) a nonelectron-withdrawing substituent (e.g., an alkyl group) on C2' or C3' tends to attain a pseudoequatorial location on the furanose ring, presumably since this arrangement minimizes unfavorable steric interactions and (ii) an electronegative substituent (e.g., OH, F) on C2' or C3' prefers a pseudoaxial location; this geometry is energetically favorable since a near-gauche arrangement with respect to the endocyclic oxygen O4' is then achieved (gauche effect).[5]

In the present work we focus on the conformational properties of the isomeric C2'/C3' modified uridines **1**–**4** (Chart I) which

Table I. Assignments of the ¹H NMR Resonances in Compounds **1**–**4**[a]

	compd 1	compd 2	compd 3	compd 4
H(1')	6.204	5.760	5.916	5.738
H(2'/2")[b]	2.936	4.646	2.974	4.714
H(3'/3")[b]	4.704	3.046	4.684	2.632
H(4')	4.030	4.196	3.966	4.040
H(5')	3.820	3.946	4.078	3.896
H(5")	3.750	3.644	4.030	3.866
H(a)	4.060	4.060	3.944	3.934
H(b)	3.620	3.576	3.342	3.376
H(c)	2.604	2.570	1.986	2.342
Me	1.110	1.050	1.050	1.078
H(5)	5.782	5.696	5.748	5.676
H(6)	8.000	7.820	7.810	7.550

[a] Chemical shifts are given in ppm, relative to TMS. Sample conditions: temperature, 25 °C; solvent, CDCl₃–CD₃OD (9:1), concentration, 20–25 mM. [b] H(2') and H(3') refer to compounds 1 and 2 (B ring on the α-face); H(2") and H(3") refer to compound 3 and 4 (B ring on the β-face).

were synthesized recently in our laboratory.[3h] The key step in these preparations is an intramolecular free radical cyclization

(1) (a) Nucleoside Analogues. Chemistry, Biology and Medical Applications. Walker, R. T., de Clercq, E., Eckstein, F., Eds.; Plenum Press: New York, 1979. (b) Y. Mizuno In *The Organic Chemistry of Nucleic Acids*; Elsevier Scientific Publishers: Amsterdam, 1985. (c) Bloch, A. *Ann. N.Y. Acad. Sci.* **1975**, *225*. (d) Suhadolnik, R. J. In *Nucleosides as Biological Probes*; Wiley: New York, 1979. (e) Review series: *Advances in Cyclic Nucleotide Research*; Greengard, P., Robinson, G. A., Sr., Eds.; Raven Press: New York, 1980–1986. (f) Agris, P. F. In *The Modified Nucleosides of Transfer RNA*; Liss, A. R. New York, 1980. (g) Proceedings of the 9th International Round Table on Nucleosides, Nucleotides and Their Biological Applications. Uppsala, Sweden, 1990. *Nucleosides and Nucleotides* **1991**, *10*, 3–737.
(2) (a) Mitsuya, H.; Yarchoan, R.; Broder, S. *Science* **1990**, *249*, 1533. (b) Yarchoan, R.; Broder, S. *Pharmacol. Ther.* **1989**, *40*, 329. (c) Martin, J. C. In *Nuceotide Analogues as Antivirial Agents*; ACS Symposium Series, No. 401, American Chemical Society: Washington, DC, 1989.

[†] Uppsala University.
[‡] The Institute of Cancer Research.

2688 *J. Am. Chem. Soc., Vol. 114, No. 7, 1992*

Koole et al.

Scheme I. Reaction Equation for the Radical Cyclizations Leading to Structures 1–4[a]
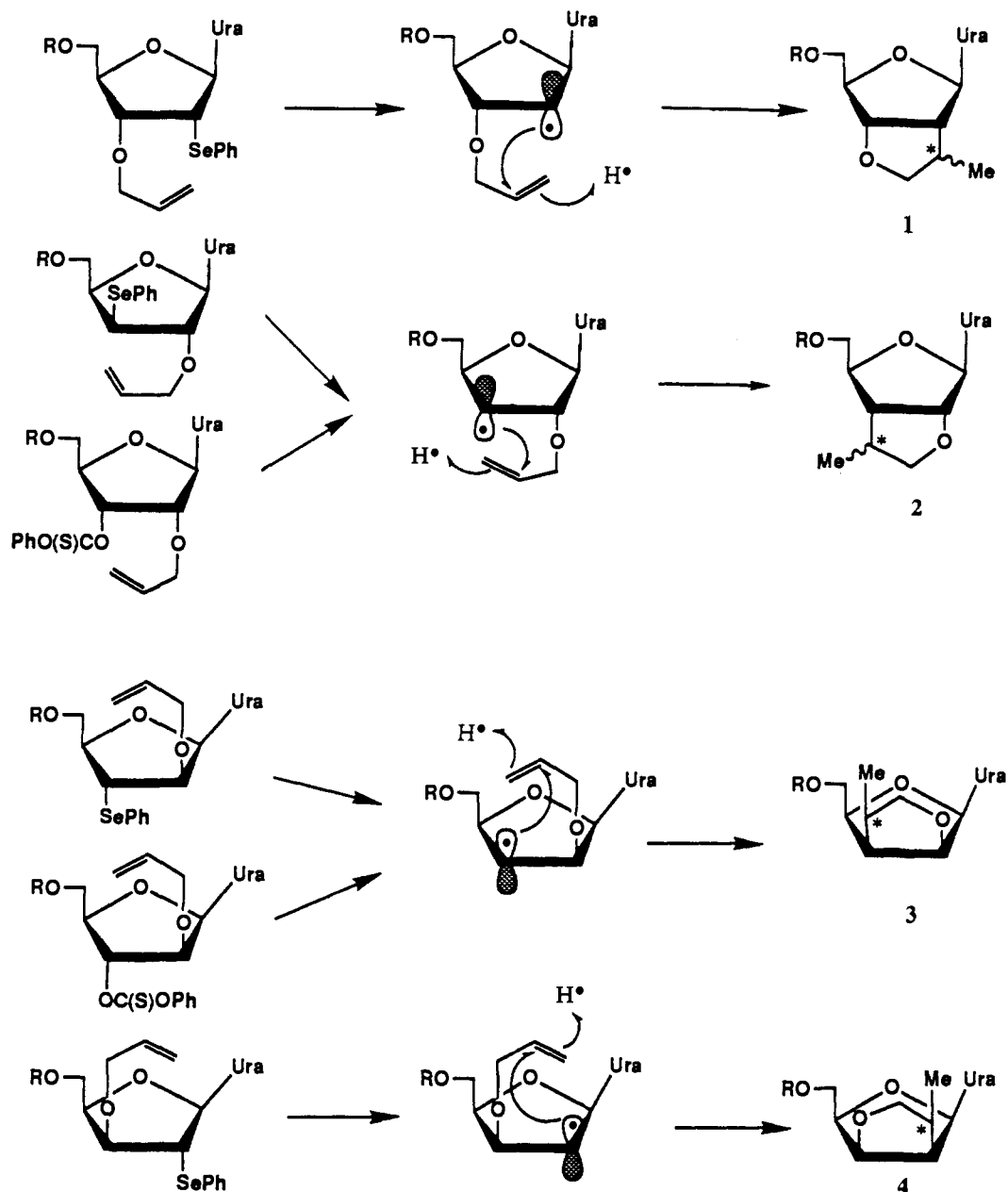
[a] It is indicated that both ring closures on the α-face (affording 1 and 2) proceed with <100% stereoselectivity, whereas both reaction on the β-face are 100% stereoselective (see text and ref 3h). Also, it is indicated for 2 and 3 that the course of the reaction is identical, irrespective of the radical precursor used. In all reactions, it holds that R = monomethoxytrityl, Ura – 1-uracil.

(Scheme I). Structures 1–4 feature a second furanose ring which bridges C2′ and C3′, either via the α-face (1 and 2) or via the β-face (3 and 4). The structural studies on 1–4 encompass determination of the stereochemical configuration on Cc, using NOE

(3) (a) Grouiller, A.; Essadiq, H.; Pacheco, H.; Juntunen, S.; Chattopadhyaya, J. *Angew. Chem., Int. Ed. Engl.* **1985**, *24*, 52. (b) Bazin, H.; Chattopadhyaya, J. *Chem. Scr.* **1986**, *26*, 13. (c) Koole, L. H.; Buck, H. M.; Bazin, H.; Chattopadhyaya, J. *Tetrahedron* **1987**, *43*, 2989. (d) Koole, L. H.; Moody, H. M.; Buck, H. M.; Grouiller, A.; Essadiq, H.; Vial, J.-M.; Chattopadhyaya, J. *Recl. Trav. Chim. Pays-Bas* **1988**, *107*, 343. (e) Vial, J.-M.; Koole, L. H.; Buck, H. M.; Chattopadhyaya, J. *Acta Chem. Scand.* **1989**, *43*, 665. (f) Wu, J.-C.; Chattopadhyaya, J. *Tetrahedron* **1989**, *45*, 4507. (g) Tong, W.; Wu, J.-C.; Chattopadhyaya, J. *Tetrahedron* **1990**, *46*, 3037. (h) Wu, J.-C.; Xi, Z.; Gioeli, C.; Chattopadhyaya, J. *Tetrahedron* **1991**, *47*, 2237.

(4) Koole, L. H.; Buck, H. M.; Nyilas, A.; Chattopadhyaya, J. *Can. J. Chem.* **1987**, *65*, 2089.

(5) (a) Kirby, A. J. *The Anomeric Effect and Related Stereoelectronic Effects at Oxygen*; Springer Verlag: Berlin, 1983. (b) Wolfe, S. *Acc. Chem. Res.* **1972**, *5*, 102. (c) Brunck, T. K.; Weinhold, F. *J. Am. Chem. Soc.* **1979**, *101*, 1700.

difference spectroscopy (^{1}H NMR at 500 MHz). Subsequently, the complete set of vicinal ^{1}H–^{1}H J coupling constants was measured over a temperature range of approximately 90 deg. These data were used for pseudorotational analysis of both furanose rings. Furthermore, we report the X-ray crystal structure of compound 2, and a comparison is made between the conformation of this compound in solution and in the solid state. The present data reveal that structures 1 and 2 exhibit opposite conformational features, whereas structures 3 and 4 are involved in a (possibly complex) conformational equilibrium. It is briefly outlined that these observations are consistent with the aforementioned principles (i) and (ii).

Results and Discussion

Table I summarizes the assignments of all ^{1}H NMR resonances in 1–4. The diastereotopic protons H5′ and H5″ are tentatively assigned according to the Remin–Shugar rule,[6] i.e., δ(H5′) >

(6) Remin, M.; Shugar, D. *Biochem. Biophys. Res. Commun.* **1972**, *48*, 636.

Structural Properties of C2'/C3' Modified Uridines

J. Am. Chem. Soc., Vol. 114, No. 7, 1992 2689

Chart I. Structural Formulae of Compounds **1** and **2** (Major Diastereomers), **3**, and **4**[a]

1

2

3

4
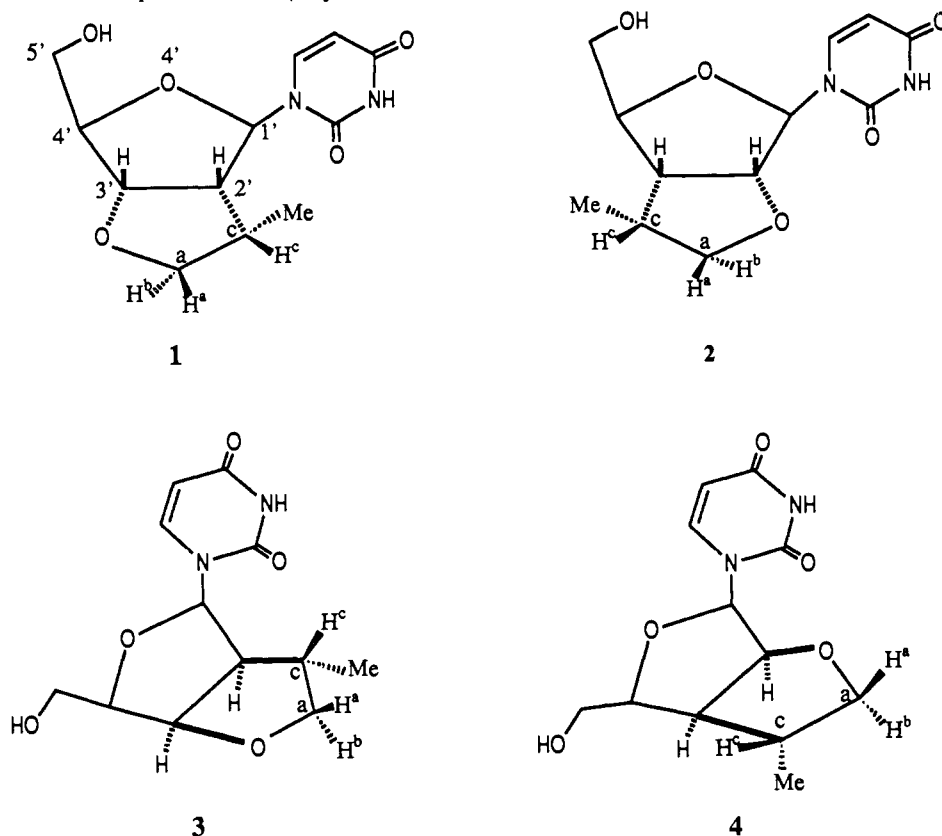
[a] Configurations on C(c) are as determined by ^{1}H NMR (1D NOE difference spectroscopy).

δ(H5''); assignment of the diastereotopic protons H^a and H^b is relatively straightforward because of the cis shielding effect of the Me group (i.e., δ(H^a) > δ(H^b) if H^a and H^b are cisoid and transoid to the Me group, respectively).[7] As can be seen in Table I, the chemical shift difference δ(H^a) − δ(H^b) is in the range 0.4–0.5 ppm, irrespective of the location of the B-ring.

A. Assignment of the Stereochemistry at Cc in 1–4. We previously stated that the radical cyclization affords compounds **1** and **2** as inseparable mixtures of diastereomers, differing with respect to the stereochemical configuration at Cc; the approximate major/minor ratios are 8:1 for **1** and 2:1 for **2**. Compounds **3** and **4**, on the other hand, were formed and isolated in stereochemically pure form. We now report the unequivocal stereochemical assignments of Cc in **1–4**, as determined by NOE difference spectroscopy (^{1}H NMR at 500 MHz).[8] Panels A(i)–F(i) in Figure 1 show relevant expansions of the NOE difference spectra, along with the corresponding unperturbed ^{1}H NMR spectra, A(ii)–F(ii). All NOE experiments refer to short irradiation of the Me resonance (see Experimental Section). For the major diastereomer of compound **1** we observed the relatively strong NOE contacts Me–H2', Me–H^b, and Me–H1', see panels A(i) and B(i) in Figure 1. These results qualitatively imply that the Me protons are relatively proximate with respect to H2', H^b, and H1'. All other protons in the molecule are so distant from the Me group, that no NOE contacts can be observed. Therefore, it can be concluded that these observations are compatible only with the Cc configuration as drawn for **1** in Chart I. In terms

of the Prelog–Ingold–Cahn convention,[9] this configuration is *R*. Thus, the minor diastereomer of **1** has *S* configuration at Cc. Panels C(i) and D(i) in Figure 1 show the analogous NOE difference spectra measured for compound **2**. Now, it it seen that saturation of the Me protons leads to the NOE enhancements Me–H3', Me–H4', Me–H5', Me–H5'', and Me–H^b. These data clearly show that the Me group in **2** resides in the vicinity of H4', H5', and H5'', i.e., the stereochemistry is as drawn in Chart I. This corresponds to *S* configuration at Cc for the major diastereomer of **2** and hence also to *R* configuration for the minor counterpart. For compound **3**, two clear NOE contacts of approximately equal intensity were found upon irradiation of the Me resonance: Me–H2' and Me–H^b, see panel E(i) in Figure 1. Hence, it can be concluded that H2' and H^b have a cisoid location with respect to the Me group, as shown in Chart I. This configuration corresponds to *R*. Similarly, it was found that saturation of the Me resonance in compound **4** produces virtually equal NOE enhancements for H3' and H^b, see panel F(i) in Figure 1. Therefore, both H3' and H^b appear to be cisoid with respect to the Me group, and the configuration at C(c) in **4** can be assigned *S*. All stereochemical Cc assignments for **1–4** are summarized in Table II.

B. Conformational Analysis of 1–4 Using ^{1}H NMR Vicinal Coupling Constants. The ribose ring and the B-ring in each of the structures **1–4** were analyzed in terms of the pseudorotation model.[10,11] The ribose conformation is defined by the phase angle

Table II. Summary of the Stereochemical Configurations at C(c) as Determined for Compounds **1** and **2** (Major and Minor Diastereomers), **3**, and **4**

compd	1 (major)	1 (minor)	2 (major)	2 (minor)	3	4
configuration at C(c)	R	S	S	R	R	S

(7) See, e.g.: Gunther, H. *NMR Spektroskopie. Eine Einfuhrung in die Protonresonanz Spektroskopie und ihre Anwendungen in der Chemie*; Georg Thieme Verlag: Stuttgart-New York, 1983. The ^{1}H NMR spectrum of 3-methyltetrahydrofuran also shows a chemical shift difference of 0.5 ppm for the diastereotopic protons, attached to C2. See: Aldrich Catalogue of Proton NMR Spectra, Section Nonaromatic Ethers M8,235-3.

(8) NOE difference spectroscopy is a powerful and frequently used tool in conformational studies of, e.g., nucleosides and nucleotides. See, e.g.: Neuhaus, D.; Williamson, M. *The Nuclear Overhauser Effect in Structural and Conformational Analysis*; Verlag Chemie: Weinheim, 1989.

(9) Cahn, R. S.; Ingold, C. K.; Prelog, V. *Angew. Chem., Int. Ed. Engl.* **1966**, *5*, 385.

Chart II. Definition of Endocyclic Torsion Angles for the Ribose and B-rings in Structures **1–4**

Ribose ring in **1 - 4**   B-ring in **1** (major diastereomer) and **3**   B-ring in **2** (major diastereomer) and **4**

$\nu_0 = [C4'-O4'-C1'-C2']$
$\nu_1 = [O4'-C1'-C2'-C3']$
$\nu_2 = [C1'-C2'-C3'-C4']$
$\nu_3 = [C2'-C3'-C4'-O4']$
$\nu_4 = [C3'-C4'-O4'-C1']$

$\tau_0 = [C3'-O-C(a)-C(c)]$
$\tau_1 = [O-C(a)-C(c)-C2']$
$\tau_2 = [C(a)-C(c)-C2'-C3']$
$\tau_3 = [C(c)-C2'-C3'-O]$
$\tau_4 = [C2'-C3'-O-C(a)]$

$\tau_0 = [C2'-O-C(a)-C(c)]$
$\tau_1 = [O-C(a)-C(c)-C3']$
$\tau_2 = [C(a)-C(c)-C3'-C2']$
$\tau_3 = [C(c)-C3'-C2'-O]$
$\tau_4 = [C3'-C2'-O-C(a)]$

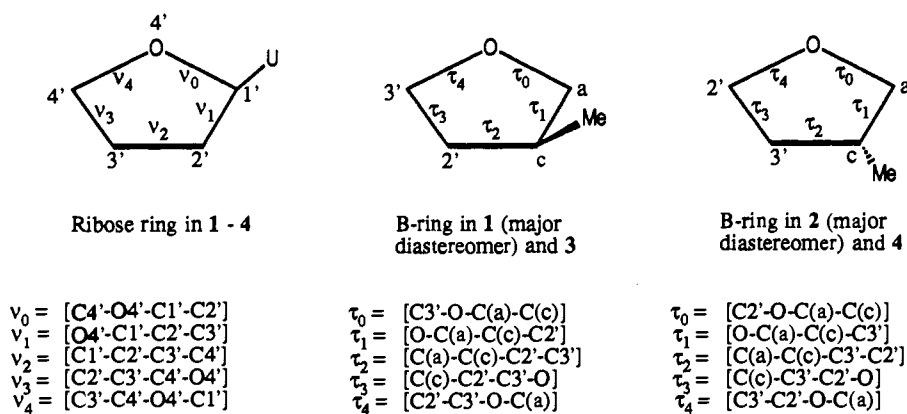**Table III.** Geometric Data Obtained from a Set of Crystal Structures of Nucleosides and Nucleotides with a Five-Membered Ring Bridging C2′ and C3′[e]

code	compd name	P	ν_m	Q	τ_m	ref
	2′,3′-Acetals					
A	2′,3′-*O*-methoxymethylene uridine	162.8	23.1	354.2	32.2	13 (a)
B	2′,3′-*O*-isopropylidene adenosine (molecule B)	215.3	31.5	3.9	35.5	13 (b)
C	8-bromo-2′,3′-*O*-isopropylidene adenosine (molecule II)	325.6	27.3	195.3	34.6	13 (c)
D	1-(5′-*O*-acetyl-2′,3′-*O*-isopropylidene-β-D-ribofuranosyl)-5-(ditosylamino)imidazole-4-carbonitrile	37.0	24.6	248.9	32.6	13 (d)
E	5′-*O*-acetyl-2′,3′-*O*-isopropylidene uridine	352.9	16.8	271.0	36.4	13 (e)
F	2′,3′-*O*-cyclohexylidene-4′-*C*-(2-methyl-2-propenyl) uridine	107	27	335	23	13 (f)
G	5′-*O*-tosyl-2′,3′-*O*-isopropylidene uridine	16.4	20.5	263.3	30.4	13 (g)
H	5-bromo-2′,3′-*O*-isopropylidene uridine	216.6	19.9	338.5	33.8	13 (h)
I	4-chloro-6-(2′,3′-*O*-isopropylidene-5′-*O*-trityl-α-D-ribofuranosylchloromethyl)-2-methylpyrimidine	217.7	19.0	339.8	28.6	13 (i)
J	2′,3′-*O*-isopropylidene uridine	216.3	23.7	340.3	33.4	13 (j)
K	2′,3′-*O*-isopropylidene guanosine[a]	196.4	25.7	350.2	38.4	13 (k)
	2′,3′-Cyclic Phosphates					
L	uridine-2′,3′-*O,O*-cyclophosphorothioate[b]	260.7	22.6	305.1	13.4	13 (l)
M	cytidine-2′,3′-cyclophosphate[c]	81.2	36.2	142.6	26.3	13 (m)
N	cytidine-2′,3′-cyclophosphate[d]	173.6	29.3	10.1	34.4	13 (n)
	C5′ to Base Cyclized Nucleosides					
O	2,5′-anhydro-1-(2′,3′-*O*-isopropylidene-β-D-ribofuranosyl)-2-thiouracil	250.6	35.4	322.5	34.8	13 (o)
P	2,5′-anhydro-2′,3′-*O*-isopropylidene cyclouridine	255.0	40.9	319.3	37.7	13 (p)
Q	6,5′-anhydro-6-hydroxy-2′,3′-*O*-isopropylidene uridine (molecule A)	258.3	38.2	316.0	37.0	13 (q)
R	6,5′-anhydro-6-hydroxy-2′,3′-*O*-isopropylidene uridine (molecule B)	254.6	40.5	326.4	30.1	13 (q)
S	6,5′-cyclo-5′-deoxy-2′,3′-*O*-isopropylidene uridine	266.2	47.7	323.0	21.4	13 (r)
T	5′-deoxy-5′,6-epithio-5,6-dihydro-2′,3′-*O*-isopropylidene-3-methyl uridine	253.8	29.2	315.0	37.1	13 (s)
U	5′-deoxy-5′,6-epithio-5,6-dihydro-2′,3′-*O*-isopropylidene uridine (molecule B)	254.6	27.4	310.9	35.1	13 (t)
V	5′-deoxy-5′,6-epithio-5,6-dihydro-2′,3′-*O*-isopropylidene uridine (molecule A)	249.4	28.8	85.9	19.3	13 (t)

[a] Dimethyl sulfoxide solvate. [b] Triethylammonium salt. [c] Sodium salt. [d] Free acid. [e] Three classes of compounds were distinguished: 2′,3′-acetals (A–K), 2′,3′-cyclic phosphates (L–N), and nucleosides incorporating a 2′,3′ acetal group while the base is bridged to C5′ (O–V).

P and the maximum puckering amplitude ν_m; the B-ring is analogously defined by the phase angle *Q* and the maximum puckering amplitude τ_m. The detailed descriptions of the respective endocyclic torsion angles are presented in Chart II. Standard nomenclature for nucleosides and nucleotides was used for the ribose ring, while the five endocyclic torsion angles in the B-ring were numbered τ_0, ..., τ_4 starting from oxygen in the direction of the Me group. Note that the atom sequence in the B-ring is O–Ca–Cc–C2′–C3′ for structures **1** and **3** and O–Ca–Cc–C3′–C2′ for structures **2** and **4** (Chart II).

According to the pseudorotation model, we can write $\nu_i = \nu_m \cos (P + (i - 2)144°)$, with $i = 0, ..., 4$, and also $\tau_j = \tau_m \cos (Q + (j - 2)144°)$, with $j = 0, ..., 4$. It is of interest to focus on the C2′–C3′ bond, which is part of both rings: $\nu_2 = [C1'-C2'-C3'-C4']$ and

$\tau_3 = [Cc-C2'/3'-C3'/2'-O]$. As a first approximation, ν_2 can be set equal to τ_3, which leads to eq 1:
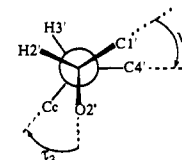
$$\tau_m = (\nu_m \cos P)/\cos (Q + 144°) \qquad (1)$$

Figure 2 is a graphical representation of eq 1.[12] The horizontal curves l_1 and l_2 were calculated for $\nu_m = 10°$ and $\tau_m = 45°$, while the vertical curves m_1 and m_2 correspond to $\nu_m = 45°$ and $\tau_m = 10°$. It follows that the shaded regions correspond to either ν_m

(10) (a) Kilpatrick, J. E.; Pitzer, K. S.; Spitzer, R. *J. Am. Chem. Soc.* **1947**, *69*, 2438. (b) Altona, C.; Sundaralingam, M. *J. Am. Chem. Soc.* **1972**, *94*, 5394; **1973**, *95*, 2333.

(11) (a) Saenger, W. *Principles of Nucleic Acid Structure*; Springer Verlag: New York, 1984. (b) Altona, C. *Recl. Trav. Chim. Pays-Bas* **1982**, *101*, 413. (c) Davies, D. B. *Progress in NMR Spectroscopy*; Emsley, J. W., Feeney, J., Sutcliffe, L. H., Eds.; Pergamon: Oxford, 1978; Vol. 12.
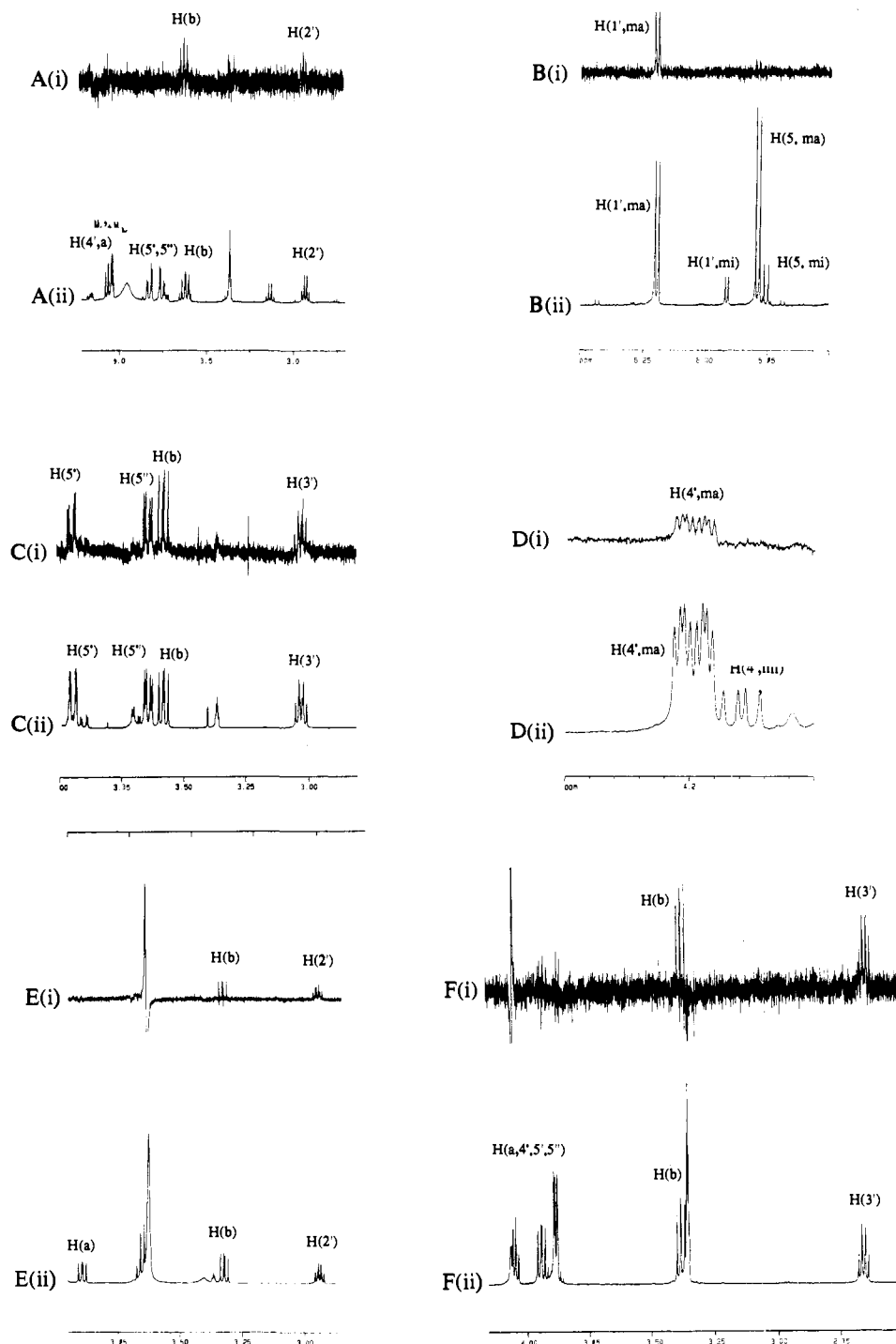
(12) The approximate equality of $\nu 2$ and $\tau 3$ is readily seen from the Newman projections along the C2′–C3′ bond. These are shown for compounds **1** and **2**. The torsion angles $\nu 2$ and $\tau 3$ are only approximately equal, since C2′ and C3′ deviate from perfect tetrahedral geometry.
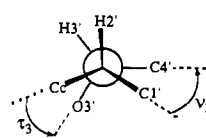
Newman projection along C2′-C3′ in **1**   Newman projection along C2′-C3′ in **2**

Figure 1. Expansions of the 500 MHz ^{1}H NMR 1D NOE difference spectra and the off-resonance spectra of compounds 1–4. All experiments refer to irradiation of the Me resonance (see Experimental Section); NOE effects for the other proton resonances were monitored. Panels A and B summarize the 1D NOE measurements on compound 1; B and D are expansions of the unperturbed (off-resonance) 1D NMR spectrum of 1; expansions (i) were obtained upon subtraction of the on- and off-resonance spectra. Clear NOE effects could be measured for H(b) and H(2') (A(i)) as well as for H1' of the major diastereomer (B(i)). From these data, it can be concluded that the Me group in the major diastereomer of 1 points backwards (*R* configuration), as shown in Chart I. Panels C and D analogously refer to compound 2. In this case, clear NOE contacts were found between the Me group and H^b, H5', H5'', and H3' (C(i)). Panel D shows the expansions of the H4' region in 2; H4' of the minor diastereomer resonates slightly upfield from H4' of the major diastereomer. While the Me resonances of both diastereomers are isochronous (i.e., simultaneous irradiation was possible), it is clearly seen that only H4' of the major diastereomer is affected (D(i)). This is a strong argument for the *S* stereochemical assignment on C(c) in the major diastereomer of 2 (Chart I), which was found in the X-ray crystal structure. Panel E refers to compound 3. In this case, we observed clear NOE contacts Me–H^b and Me–H2'. Note that no NOE effect can be detected between Me and the transoid vicinal proton H^a. These data reveal a cisoid orientation of the Me group and H2', i.e., the Me group has outward location (*R* configuration) as shown for 3 in Chart I. The relatively large dispersive signal in panel I is due to the residual peak of the hydroxylic protons. Panel F corresponds to compound 4. Now, clear NOEs are Me–H^b and Me–H3', showing again an outward orientation of the Me group (*S* configuration, see Chart I). Note that no NOE effects could be detected for the protons H^a, H4', H5', and H5''.

or $\tau_m < 10°$ or $>45°$, and therefore these conformational regions are considered inaccessible. There is no a priori evidence that ν_m and τ_m must lie in the range 10°–45°, but it is known that

C2',C3' bridged nucleosides and nucleotides usually have puckering amplitudes within this range. This is apparent from a compilation of 22 relevant X-ray crystal structures (Table III).[13] The con-

Table IV. J Coupling Constants (Hz), Measured for Compounds **1** and **2** (Major Diastereomers), **3**, and **4** at Different Sample Temperatures[g]

coupling	compd 1			compd 2				compd 3			compd 4			
	243 K	300 K	323 K	243 K	273 K	293 K	333 K	243 K	293 K	333 K	233 K	243 K	300 K	333 K
$J_{1'2'}$[a]	7.8	7.6	7.3	1.0	1.0	1.0	1.6	6.6	6.7	6.7	3.9	3.9	3.9	3.9
$J_{2'3'}$[b]	6.4	6.6	6.7	6.6	6.5	6.5	6.5	6.5	6.5	6.55	7.2	7.3	7.3	7.2
$J_{3'4'}$[c]	2.1	2.5	2.6	9.0	9.1	8.9	8.8	3.6	3.6	3.65	6.0	6.0	6.0	6.0
$J_{4'5'}$	2.3	2.8	3.0	2.1	2.2	2.3	2.5	3.8	4.6	f	3.3	3.8	5.2	f
$J_{4'5''}$	2.8	3.0	3.3	4.1	4.0	3.9	4.2	7.3	4.4	f	8.3	8.2	6.7	f
$J_{2'c}$[d]	6.7	6.8	7.1					4.3	4.3	4.2				
$J_{3'c}$[e]				6.3	6.45	6.6	6.5				6.5	6.4	6.4	6.1
J_{ac}	7.7	7.6	7.8	10.9	10.9	10.8	10.6	6.8	7.0	7.0	6.2	6.1	6.3	6.4
J_{bc}	11.3	10.6	10.4	7.6	7.6	7.6	7.5	6.7	6.8	6.9	7.6	7.4	7.5	7.4
J_{ab}	8.5	8.5	8.5	8.5	8.5	8.5	8.5	8.5	8.5	8.5	8.5	8.5	8.5	8.5
$\gamma(+)$	84	78	73	70	70	73	68	20	47	f	17	14	17	f
$\gamma(t)$	16	17	20	30	30	27	32	68	27	f	74	71	50	
$\gamma(-)$	0	5	7	0	0	0	0	12	26	f	9	15	33	

[a] $J_{1'2'}$ in the case of **3** and **4**. [b] $J_{2'3''}$ in the case of **3** and **4**. [c] $J_{3''4'}$ in the case of **3** and **4**. [d] $J_{2''c}$ in the case of **3**. [e] $J_{3''c}$ in the case of **4**. [f] Could not be determined. [g] Calculated relative populations of the $\gamma(+)$, $\gamma(t)$, and $\gamma(-)$ rotamers about the C4'-C5' bond are also given.

formations of these systems are depicted in the Q vs P plot of Figure 2 and fall without exception within the nonshaded regions. Most importantly, Figure 2 pictures a conformational correlation between the ribose ring and the B-ring in **1-4**: if the ribose ring adopts a North-type conformation (P around 0°), then the B-ring will assume a South-type conformation (Q around 200°) and vice versa. This qualitative correlation proved very useful during setup and evaluation of our conformational analyses of **1-4** (vide infra).

The NMR conformational analyses on **1-4** are based on the set of vicinal $^1H-^1H$ J coupling constants, which are compiled in Table IV. Our method will be outlined in detail for the conformational analysis of the ribose ring in structure **1**. Three coupling constants, i.e., $J_{1'2'}$, $J_{2'3'}$, and $J_{3'4'}$ are available. It is important to realize that two essential working hypotheses need to be invoked. The first concerns translation of the experimentally determined J couplings into the corresponding proton-proton torsion angles θ_{HH}. For this, we have used the well-known generalized Karplus equation as developed by Altona et al.[14] The second hypothesis concerns the translation of the ϕ_{HH} values into the corresponding endocyclic torsion angle ν_j. For this, we used simple linear relationship of the form $\phi_{HH} = A + B\nu_j$, using parameters A and B as obtained by Altona et al. from a statistical survey of 178 X-ray crystal structures of nucleosides and nucleotides.[15] Thus, *three inevitable sources of inaccuracy are associated with our conformational analysis*: one stems from
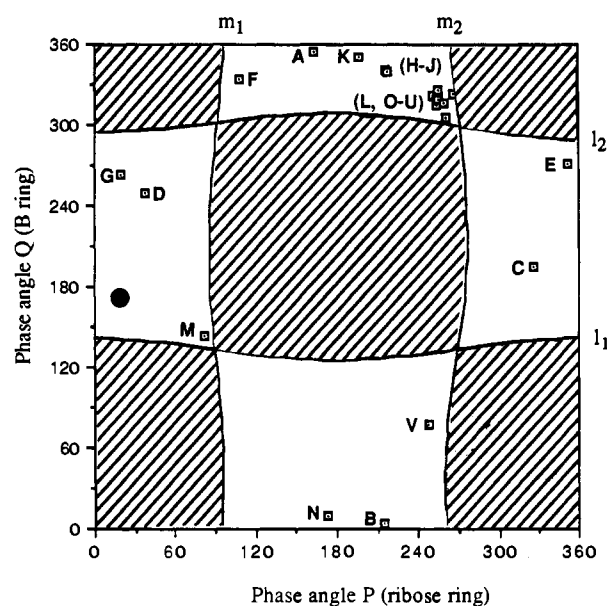

Figure 2. Visualization for formula **1**. The horizontal sinoid curves (I_1 and I_2) were calculated for $\nu_m = 10°$ and $\tau_m = 45°$, while the vertical sinoids (m_1 and m_2) were calculated for $\nu_m = 45°$ and $\tau_m = 10°$. The shaded regions in this graph were considered inaccessible, since either ν_m or τ_m are then $<10°$ or $>45°$, i.e., the puckering amplitudes are then excessively low or high. (P,Q) Points abstracted from 22 crystal structures (coded A-V) are shown to fall in the nonshaded regions (codes A-V, see Table III). The numbering of the endoxcyclic torsion angles in the B-ring of structures V is as follows: $\tau_0 = [C2'-O2'-C*-O3']$, $\tau_1 = [O2'-C*-O3'-C3']$, $\tau_2 = [C*-O3'-C3'-C2']$, $\tau_3 = [O3'-C3'-C2'-O2']$, and $\tau_4 = [C3'-C2'-O2'-C*]$, i.e., analogous to the numbering used in structure **2**. The (P,Q) obtained from crystal structure of compound **2** ($P = 26°$ and $Q = 175°$) also falls within a nonshaded region, as indicated by a black dot. The correlation between P and Q, as depicted in this figure proved useful in the interpretation of the data as obtained from NMR experiments (see text). Note that the data points on the base-to-C5' bridged structures O-V (Table III) nearly coincide, one notable exception is structure V (see also ref 13t). Note also that molecule A of 2'-O-isopropylidene adenosine (ref 13b) and molecule I of 8-bromo-2',3'-O-isopropylidene adenosine (ref 13c) were omitted from the plot, since the ribose rings in these structures were found to be virtually flat, which precludes accurate determination of the phase angle.

(13) (a) de Kok, A. J.; Romers, C.; de Leeuw, H. P. M.; Altona, C.; van Boom, J. H. *J. Chem. Soc., Perkin Trans II* **1977**, 487. (b) Sprang, S.; Rohrer, D. C.; Sundaralingam, M. *Acta Crystallogr.* **1978**, *B34*, 1803. (c) Fujii, S.; Fujiwara, T.; Tomita, K.-I. *Nucl. Acids Res.* **1976**, *3*, 1985. (d) Kitamura, K.; Mizuno, H.; Sugio, S.; Okabe, N.; Ikehara, M.; Tomita, K.-I. *Acta Crystallogr.* **1983**, *C39*, 1551. (e) Seshadri, T. P.; Gautham, N.; Viswamitra, M. A. *Acta Crystallogr.* **1983**, *C39*, 1706. (f) Cook, W. J.; Ealick, S. E.; Secrist III, J. A. *Acta Crystallogr.* **1984**, *C40*, 885. (g) Gautham, N.; Seshadri, T. P.; Viswamitra, M. A. *Acta Crystallogr.* **1983**, *C39*, 459. (h) Gautham, N.; Seshadri, T. P.; Viswamitra, M. A. *Acta Crystallogr.* **1983**, *C39*, 456. (i) Katagiri, N.; Takashima, K.; Kato, T.; Sato, S.; Tamura, C. *J. Chem. Soc., Perkin Trans. I* **1983**, 201. (j) Katti, S. K.; Seshadri, T. P.; Viswamitra, M. A. *Acta Crystallogr.* **1981**, *B37*, 407. (k) Mande, S. S.; Seshadri, T. P.; Viswamitra, M. A. *Acta Crystallogr.* **1988**, *C44*, 912. (l) Saenger, W.; Eckstein, F. *J. Am. Chem. Soc.* **1970**, *92*, 4712. (m) Coulter, C. L. *J. Am. Chem. Soc.* **1973**, *95*, 570. (n) Reddy, B. S.; Saenger, W. *Acta Crystallogr.* **1978**, *B34*, 1520. (o) Yamagata, Y.; Fujii, S.; Fujiwara, T.; Tomita, K.-I.; Ueda, T. *Acta Crystallogr.* **1980**, *B36*, 339. (p) Delbaere, L. T. J.; James, M. N. G. *Acta Crystallogr.* **1974**, *B30*, 1241. (q) Mande, S. S.; Seshadri, T. P.; Viswamitra, M. A. *Acta Crystallogr.* **1988**, *C44*, 138. (r) Yamagata, Y.; Tomita, K.-I.; Usui, H.; Sano, T.; Ueda, T. *Chem. Pharm. Bull.* **1989**, *37*, 1971. (s) Gautham, N.; Ramakrishnan, P.; Seshadri, T. P.; Viswamitra, M. A.; Salisbury, S. A.; Brown, D. M. *Acta Crystallogr.* **1982**, *B38*, 2707. (t) Gautham, N.; Seshadri, T. P.; Viswamitra, M. A.; Salisbury, M.; Brown, D. M. *Acta Crystallogr.* **1983**, *C39*, 1389.

(14) Haasnoot, C. A. G.; de Leeuw, F. A. A. M.; Altona, C. *Tetrahedron* **1980**, *36*, 2783.

(15) The relations used are as follows: $\phi_{1'2'} = 121.4 + 1.03 \nu_1$ in **1** and **2**, and $0.9 + 1.02 \nu_1$ in **3** and **4**, and $-4.0 + 1.09 \nu_3$ in **3** and **4**; $\phi_{2'3'} = 2.4 + 1.06 \nu_2$ in **1-4**; $\phi_{3'4'} = -124.0 + 1.09 \nu_3$ in **1** and **2**, and $-4.0 + 1.09 \nu_3$ in **3** and **4**; $\phi_{ac} = \tau_1$ in **1-4**; $\phi_{bc} = -120 + \tau_1$ in **1** and **3**, and $120 + \tau_1$ in **2** and **4**; $\phi_{2(3')c} = \tau_2$ in **1** and **2**, $120 + \tau_2$ in **3**, and $-120 + \tau_2$ in **4**; $\phi_{2'3'} = \tau_3$ in **1-4**. The relations between ϕ_{HH} and ν_i were abstracted: de Leeuw, H. P. M.; Haasnoot, C. A. G.; Altona, C. *Isr. J. Chem.* **1980**, *20*, 108.

experimental errors associated with measurement of J couplings, one is due to application of the Karplus equation, and one stems from the assumed relation between ϕ_{HH} and ν_i. This implies that there will be an ensemble of conformations that are in agreement with the set of J couplings measured on compound **1**. In order to define this ensemble, we treated the ribose conformations as a rapid equilibrium between a predominant conformer I (characterized by $P(I)$ and $\nu_m(I)$) and a minor conformer II (characterized by $P(II)$ and $\nu_m(II)$). A mole fraction $x(I)$ defines the composition of the equilibrium at each sample temperature. In
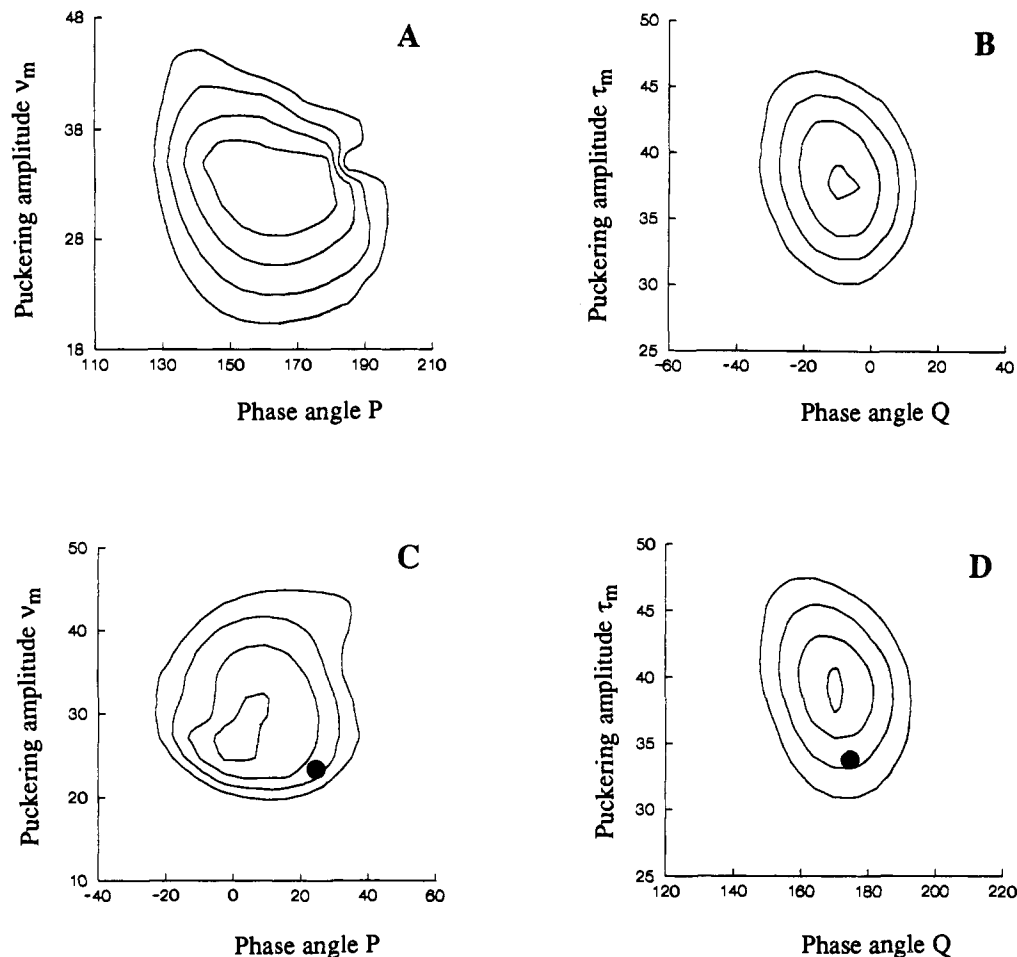
Figure 3. Rms contours as calculated with the PSEUROT program for structures **1** and **2** using the J coupling data in Table II (see text). Parts A and B correspond to the ribose and B-rings in **1**; parts C and D correspond to the ribose and B-rings in **2**. The rms values increase in the order 0.5, 0.7, 0.9, and 1.1 going from the inner to the outer contours in each graph. The points (P, ν_m) and (Q, τ_m) as abstracted from the crystal structure of **2** are shown in parts C and D, respectively. The position of these points illustrates the agreement between the conformational models as obtained by ^{1}H NMR (solution conformation) and X-ray crystallography.

the case of **1**, the predominant conformation of the ribose ring was initially chosen in the South region of the pseudorotation cycle (around $P = 180°$), based on the observation that $J_{1'2'}$ is 7.3–7.8 Hz (Table IV).[16] Subsequently, we performed a series of calculations using the PSEUROT algorithm.[17] The parameters P(I) and ν_m(I) were fixed on a fine grid in the two-dimensional conformational space $100° < P < 210°$ and $18° < \nu_m < 48°$, while the parameters P(II), ν_m(II), and x(I) were optimized as to minimize the overall root mean square (rms) error. In this way, the rms contours shown in Figure 3A were constructed. Going from the inner toward the outer contour in Figure 3A, the rms error increases from 0.5, to 0.7, to 0.9, to 1.1 Hz. It should be noted that the preference for conformer I was found to be >92% in each rms calculation. On the basis of Figure 3A, it can be safely concluded that the ribose ring in **1** assumes a South-type conformation. This conclusion remains valid even if the three sources

of inaccuracy (vide supra) would result in an overall rms error as large as ca. 1 Hz.

Conformational analysis of the B-ring in **1** was performed in essentially the same way. Now, four J couplings are available, these are J_{ac}, J_{bc}, $J_{2'c}$, and $J_{2'3'}$ (Table IV). The predominant B-ring conformation was chosen in the North region, as indicated by Figure 2. The resulting rms contours are depicted in Figure 3B; the rms values also are 0.5, 0.7, 0.9, and 1.1 Hz, going from the inner contour toward the outer. High preferences (>94%) were found for a North-type B-ring conformation in each rms calculation. Figure 3B leaves no doubt that the B-ring in structure **1** assumes a North-type conformation.

The conformational analyses of structure **2** were of particular interest, since now a comparison can be made between the results from J coupling analysis (solution conformation) and the X-ray crystal structure (vide infra). The rms contours for the ribose ring and the B-ring in **2** are shown in Figures 3 (parts C and D, respectively). These graphs show that the ribose ring in **2** resides in a North-type conformation, whereas the B-ring in **2** is in a South-type conformation. Noteworthy, the points (P, ν_m) and (Q, τ_m), as obtained from the X-ray crystal structure, fall within the rms = 0.9 Hz contour in both graphs. This means that there is a favorable agreement between the J coupling analysis and the X-crystal structure. It can also be concluded that structures **1** and **2** show completely reversed molecular conformations, as far as the furanose rings are concerned. This aspect will be further discussed below.

Pseudorotational analysis of structures **3** and **4** proved to be seriously hampered due to the fact that the experimental set of J coupling constants cannot be fitted with one particular (pre-

(16) It is well established that the conformational properties of the ribose of deoxyribose rings in nucleosides, nucleotides, and oligonucleotides in solution can be interpreted in terms of a North/South two-state equilibrium. The coupling constant $J_{1'2'}$ for ribose rings, or the sum $J_{1'2'} + J_{1'2''}$ in deoxyribose rings, can provide a fairly accurate picture of the mole fraction of, e.g., the North-type conformer. For example, it holds for ribose rings that %(North) = 100 × (7.8 − $J_{1'2'}^{exp}$)/7.3 (van den Hoogen, Y. Th.; Treurniet, S. J.; Roelen, H. C. P. F.; de Vroom, E.; van der Marel, G. A.; Van Boom, J. H.; Altona, C. *Eur. J. Biochem.* **1988**, *171*, 155). Although this equation is not directly applicable to our compounds (appropriate corrections for orientation and electronegativities of substituents are lacking), it is found that $J_{1'2'}$ also provides a rough idea of the ribose conformation in **1** and **2**. Note that only $J_{1'2''}$ is available for compounds **3** and **4**.

(17) (a) de Leeuw, F. A. A. M.; Altona, C. *J. Comput. Chem.* **1983**, *4*, 438. (b) de Leeuw, F. A. A. M.; Altona, C. QCPE Program No. 463.
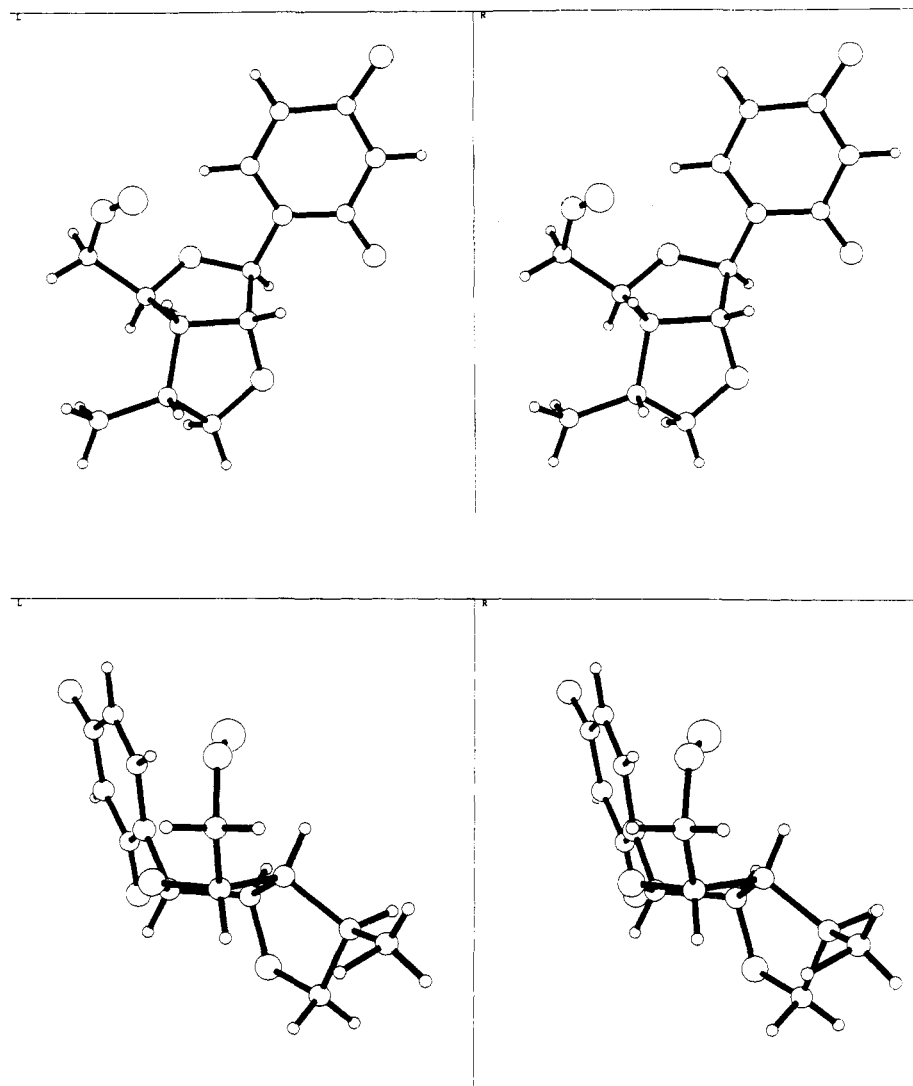
Figure 4. Stereoplots of the X-ray crystal structure of compound **2**. The structure shows a North-type puckered ribose ring and a South-type puckering of the B-ring, which is in agreement with the correlation graphs of Figure 2 and also with the NMR results.

dominant) molecular conformation, i.e., **3** and **4** are engaged in an unbiased conformational equilibrium. A further complication is that the J couplings hardly show any change as a function of the sample temperature (Table IV). Even in the simplest case of a two-state conformational equilibrium, this means that the problem is underdetermined. In order to describe such an equilibrium, we need nine parameters (i.e., P, ν_m, Q, and τ_m in forms I and II and the mole fraction of I), whereas essentially only seven observables are available. Therefore, it has to be concluded that no satisfactory description of the dynamical properties of the furanoid rings in **3** and **4** can be derived from the J coupling data. Of course, it is an interesting question why structures **1** and **2** show a conformational bias, whereas **3** and **4** do not. A possible rationale for these observations is given below.

The conformation around the exocyclic C4'–C5' (γ) bond in **1–4** could be analyzed straightforwardly on the basis of $J_{4'5'}$ and $J_{4'5''}$.[18] The results are also listed in Table IV. Compounds **1** and **2** show a preference for the $\gamma(+)$ rotamer, as is commonly encountered in free nucleosides. Compounds **3** and **4**, on the other hand, have a preference for $\gamma(t)$, which can most probably be ascribed to steric interference of the 5'-OH group with the B-ring, which is now placed on the β-face of the molecule.

C. Crystal Structure of Compound 2. Figure 4 shows the structure of compound **2**, as determined by single-crystal X-ray diffraction. The structure is only of limited accuracy due to the

(18) Haasnoot, C. A. G.; de Leeuw, F. A. A. M.; de Leeuw, H. P. M.; Altona, C. *Recl. Trav. Chim. Pays-Bas* **1979**, *98*, 576.

Table V. Positional Parameters (Structure 2) and Their Estimated Standard Deviations[a]

atom	x	y	z	B (Å²)
O2'	0.4539 (7)	0.2745 (4)	0.8681 (5)	5.9 (2)
O2	0.3808 (7)	−0.0099 (4)	0.8987 (4)	5.2 (1)
O4'	0.7697 (9)	0.1476 (4)	0.7593 (4)	4.7 (1)
O4	0.7755 (7)	−0.2505 (4)	1.0113 (5)	5.1 (1)
O5'	1.1158 (8)	0.1929 (5)	0.8434 (5)	6.7 (2)
CMe	0.796 (1)	0.4835 (7)	0.8501 (8)	6.7 (3)
N1	0.6789 (8)	0.0253 (5)	0.8780 (4)	3.3 (2)
N3	0.5836 (8)	−0.1300 (5)	0.9541 (5)	3.6 (2)
C1'	0.631 (1)	0.1208 (6)	0.8251 (6)	4.0 (2)
C2'	0.608 (1)	0.2138 (6)	0.8960 (6)	3.6 (2)
C2	0.538 (1)	−0.0358 (6)	0.9095 (6)	3.7 (2)
C3'	0.767 (1)	0.2841 (6)	0.8817 (6)	3.7 (2)
C4	0.755 (1)	−0.1629 (5)	0.9716 (6)	3.7 (2)
C4'	0.833 (1)	0.2543 (6)	0.7773 (6)	3.8 (2)
C5'	1.039 (1)	0.2535 (8)	0.7680 (8)	6.4 (3)
C5	0.897 (1)	−0.0932 (6)	0.9436 (6)	4.0 (2)
C6	0.8555 (9)	−0.0034 (6)	0.8963 (6)	3.7 (2)
Cc	0.690 (1)	0.3947 (6)	0.8922 (6)	4.5 (2)
Ca	0.501 (1)	0.3821 (6)	0.8497 (8)	5.5 (3)

[a] These atoms were refined anisotropically and given in the form of the isotropic equivalent displacement parameter defined as $(^4/_3)[a2B(1,1) + b2B(2,2) + c2B(3,3) + ab(\cos \gamma)B(1,2) + ac(\cos \beta)B(1,3) + bc(\cos \alpha)B(2,3)]$.

relatively poor quality of the crystals obtainable. However, conformational features have been clearly established. Table V lists the positional parameters. Non-hydrogen bond lengths and

Table VI. Bond Distances and Bond Angles in the Crystal Structures of **2**[a]

Bond Distances (Å)

atom 1	atom 2	distance	atom 1	atom 2	distance	atom 1	atom 2	distance
O(2')	C(2')	1.435 (9)	C(Me)	C(c)	1.50 (1)	C(2')	C(3')	1.49 (2)
O(2')	C(a)	1.44 (1)	N(1)	C(1')	1.45 (1)	C(3')	C(4')	1.53 (2)
O(2)	C(2)	1.22 (1)	N(1)	C(2)	1.37 (1)	C(3')	C(c)	1.53 (2)
O(4')	C(1')	1.40 (2)	N(1)	C(6)	1.386 (9)	C(4)	C(5)	1.43 (1)
O(4')	C(4')	1.459 (9)	N(3)	C(2)	1.38 (1)	C(4')	C(5')	1.55 (1)
O(4)	C(4)	1.25 (1)	N(3)	C(4)	1.36 (2)	C(5)	C(6)	1.34 (2)
O(5')	C(5')	1.39 (1)	C(1')	C(2')	1.53 (1)	C(c)	C(a)	1.53 (1)

Bond Angles (deg)

atom 1	atom 2	atom 3	angle	atom 1	atom 2	atom 3	angle
C(2')	O(2')	C(a)	111.4 (6)	C(2')	C(3')	C(c)	104.1 (6)
C(1')	O(4')	C(4')	111.1 (6)	C(4')	C(3')	C(c)	115.6 (6)
C(1')	N(1)	C(2)	115.8 (7)	O(4)	C(4)	N(3)	117.7 (7)
C(1')	N(1)	C(6)	122.9 (7)	O(4)	C(4)	C(5)	125.3 (8)
C(2)	N(1)	C(6)	121.3 (6)	N(3)	C(4)	C(5)	117.0 (6)
C(2)	N(3)	C(4)	124.8 (6)	O(4')	C(4')	C(3')	106.2 (6)
O(4')	C(1')	N(1)	109.2 (6)	O(4')	C(4')	C(5')	107.5 (6)
O(4')	C(1')	C(2')	106.5 (6)	C(3')	C(4')	C(5')	113.2 (7)
N(1)	C(1')	C(2')	111.7 (6)	O(5')	C(5')	C(4')	110.7 (7)
O(2')	C(2')	C(1')	110.0 (6)	C(4)	C(5)	C(6)	119.0 (7)
O(2')	C(2')	C(3')	106.0 (6)	N(1)	C(6)	C(5)	121.6 (7)
C(1')	C(2')	C(3')	107.4 (6)	C(Me)	C(c)	C(3')	117.8 (8)
O(2)	C(2)	N(1)	122.7 (7)	C(Me)	C(c)	C(a)	115.2 (7)
O(2)	C(2)	N(3)	121.4 (8)	C(3')	C(c)	C(a)	102.4 (6)
N(1)	C(2)	N(3)	116.0 (7)	O(2')	C(a)	C(c)	105.1 (6)
C(2')	C(3')	C(4')	102.8 (6)				

[a] Numbers in parentheses are estimated standard deviations in the least significant digits.

Table VII. Selected Set of Torsion Angles in the Crystal Structure of **2**

[O5'–C5'–C4'–C3']	51.5 (9)	[C3'–C4'–O4'–C1']	18.0 (8)
[C6–N1–C1'–C2']	–89.7 (8)	[C2'–O–Ca–Cc]	–13.5
[C4'–O4'–C1'–C2']	–3.9 (8)	[O–Ca–Cc–C3']	28.4 (8)
[O4'–C1'–C2'–C3']	–12.1 (8)	[Ca–Cc–C3'–C2']	–32.9 (8)
[C1'–C2'–C3'–C4']	22.0 (8)	[Cc–C3'–C2'–O]	25.6 (8)
[C2'–C3'–C4'–O4']	–24.2 (8)	[C3'–C2'–O–Ca]	–7.7 (9)

bond angles are presented in Table VI, and a selected set of torsion angles is compiled in Table VII. As can be seen in Figure 4, the ribose ring in **2** adopts a North-type conformation. The pseudorotational parameters are $P = 26°$ and $\nu_m = 25°$. The glycosyl bond length C1'–N1 and bond angle O4'–C1'–N1 are 1.45 (1) Å and 109.2 (6)°, respectively. The conformation of the glycosidic bond is anti, with a value of –89.7 (8)° for χ[C6–N1–C1'–C2'], this is well within the common anti domain.[11a] The conformation around the C4'–C5' bond is γ(+), with γ[O5'–C5'–C4'–C3'] = 51.5 (9)°. The B-ring has the S conformation at Cc, which is in agreement with our assignment on the basis of NOE difference ¹H NMR spectroscopy (vide supra, Table II). The pseudorotational parameters, i.e., the phase angle Q and the maximum puckering amplitude, are 175° and 33°, respectively. This pucker can be designated as South-type, which fits satisfactorily with the qualitative correlations between P and Q, as depicted in Figure 2.

Concluding Remarks

As mentioned above, compounds **1** and **2** are formed and isolated as mixtures of diastereomers, with different configurations at Cc. Compounds **3** and **4**, on the other hand, are formed with 100% stereoselectivity. These observations provide indirect information about the course of the radical reaction that leads to the closure of the B-ring (Scheme II). With respect to the formation of **2** and **3**, it was verified experimentally that the stereochemical outcome is identical when a phenylselenyl or a phenylthiocarbonate group is used to generate the radical on C3'[3h]. These results imply that a relatively late transition state is involved, i.e., thermodynamic control over the stereoselectivity is to be expected. Molecular models of **3** and **4** show that inversion of configuration at Cc leads to severely crowded structures. For **3**, this means that close contact between the Me group and the uracil base is unavoidable; for **4**, it is seen that the Me group is forced in close proximity with respect to the 5'-OH group. Thus, molecular models of **3** and **4** readily illustrate why these structures have outward orientation of the Me group (i.e., R and S configuration at Cc, respectively). For structures **1** and **2**, however, molecular models do not explain the observed stereoselectivities. Contrary to what might be expected on the basis of steric repulsion arguments, *inward* location of the Me groups is encountered in the major diastereomers of **1** and **2**.

Structure **1** shows a South-type conformation for the ribose ring, which corresponds with pseudoequatorial location of Ca and pseudoaxial location of O3'. Such a conformation is favorable for at least two reasons (vide supra), i.e., (i) release of steric hindrance associated with pseudoequatorial location of Ca and (ii) the gauche effect of pseudoaxial O3' and endocyclic O4'.[4,5] These two factors can have a pronounced affect on the conformation of furanose rings, especially if they work in the same direction, as is clearly the case for the South-puckered ribose ring in **1**. It is now of interest to examine the B-ring, which is in a North-type conformation. It is readily seen that the R configuration on Cc places the CH₂• radical in the pseudoequatorial position with respect to the B-ring (favorable), whereas the S configuration on Cc corresponds with the pseudoaxial location of CH₂• (unfavorable). This may explain the observed stereoselectivity of the radical ring closure reaction during the formation of **1**. *The stereoselectivity thus seems to be imposed by the conformational preferences of the modified ribose ring.*

The same line of reasoning can be followed to explain the conformational preference of compound **2**. Now, a preference for a North-type conformation of the ribose ring is found, which corresponds with the combined pseudoaxial location of O2' and pseudoequatorial location of Ca. The B-ring has to assume a South-type conformation (viz. Figure 2). Then, the S configuration on Cc places CH₂• in the most favorable pseudoequatorial location, and this configuration is indeed encountered in the major diastereomer of **2**. It should be noted, however, that the preference of S over R configuration in **2** (i.e., approximately 2:1) is less pronounced than the preference of R over S in compound **1** (i.e., approximately 8:1).

Interestingly, the dynamic behavior of compounds **3** and **4** can also be rationalized in terms of the same model description. The ribose rings of **3** and **4** are expected to show conformational preferences for North- and South-type conformations, respectively,

and the B-ring conformations should consequently fall in the South and North regions, respectively. A conflict of interest arises at this point, since the pseudoequatorial location would imply that CH_2^* points *inward*, both for **3** and **4**. This, however, leads to highly unfavorable steric interactions with either the uracil base (in **3**) or the bulky 5'-*O*-monomethoxytrityl group (in **4**). It can be concluded that structures **3** and **4** represent nonoptimal combinations of preferred ribose conformation on one hand and Cc configuration on the other hand. This may explain why a possibly complex conformational equilibrium is encountered for **3** and **4**, instead of a bias to one particular molecular conformation.

Experimental Section

^{1}H NMR measurements were performed on a Bruker AMX 500 spectrometer. A mixture of $CDCl_3$ and CD_3OD (90:10) was used as the solvent. The sample temperature was controlled within an range of approximately 0.2 centigrades. Sample concentrations were in the range 20–25 mM. All compounds were measured under identical spectral and processing conditions: 5000 Hz sweep width, 32K time domain, zero-filling to 64K, and slight apodization (resolution enhancement with linebroadening of $\sim$1 Hz). Virtually all subspectra were found to be first-order, which facilitated extraction of J coupling constants and chemical shifts. Some spectral patterns were simulated and a standard computer simulation algorithm. One-dimensional NOE experiments were run with 2 s of irradiation time, and a decoupling power of 50 dB below 0.2 W. NOE difference spectra were obtained upon subtraction of on- and off-resonance spectra after identical line broadening (0.25 Hz exponential multiplication) and Fourier transformation.

Crystals of **2** were obtained as small thin platelets after crystallization from aqueous alcohol. Cell dimensions are a = 7.438 (2) Å, b = 12.737 (2) Å, c = 13.438 (3) Å, from least-squares refinement of 25 Θ values measured on a CAD4 diffractometer. The space group was $P2_12_12_1$. Intensity data were collected on a crystal of size 0.1 × 0.08 × 0.01 mm using a turbo-CAD4 diffractometer on a rotating-anode generator running at 40 kv, 60 mA with a fine-focus filament and a copper target. Graphite-monochromated Cu Kα radiation was used. Data were collected using an ω-2Θ scan technique in the range 1.5 < Θ < 60° for 0 < h < 8, 0 < k < 14 and 0 < l < 15, with a maximum count time of 120 s per reflection. The intensities of three standard reflections were monitored during the data collection; no significant decay was observed. A total of 563 reflections were considered to be observed, with $I \geq 2.5\sigma(I)$, out of 1071 unique reflections measured. The structure was solved, with

difficulty, by a combination of direct and search methods. Standard automated direct method approaches did not yield a solution. However, use of the SHELXS-86 program was successful with 60 reflections having the highest estimated α values being employed in the initial subset for the random start multisolution phasing.[19] The subsequent "best-solution" E map showed most of the structure. Its orientation and position were confirmed by search procedures.[20] The structure was refined by full-matrix least-squares methods on F. The positions of all hydrogen atoms were calculated by standard geometric considerations, except the one attached to O5'; this was located in a difference Fourier map. Their contributions were included in the structure factor calculations but not in the refinement process. This converged to a final R of 0.045 and R_w of 0.046 with weights of the form w = $1/[\sigma^2(F) + 0.04(F)^2]$. The maximum and minimum electron density levels are $\pm$0.27 e/Å^3. Coordinates are listed in Table V. Calculations were performed with the SDP package,[21] using atomic scattering factors from the *International Tables for X-ray Crystallography*. H-atom coordinates, anisotropic parameters for non-H atoms, and observed and calculated structure factors are provided as supplementary material.

Supplementary Material Available: Tables of H-atom coordinates and anisotropic parameters for non-H atoms for compound **2** (4 pages); table of observed and calculated structure factors for compound **2** (6 pages). Ordering information is given on any current masthead page.

(19) Sheldrick, G. M. The SHELXS-86 crystallographic program for the solution of crystal structures. University of Gottingen, Germany, 1986.

(20) Egert, E.; Sheldrick, G. M. *Acta Crystallogr. Sect. A* **1985**, A41, 262.

(21) Enraf-Nonius Structure Determination Package 1986; Enraf-Nonius: Delft, Holland; B. A. Frenz and Associates, College Station, TX.